Effects of Multiple Ligand Binding on Kinetic Isotope Effects in PQQ-Dependent Methanol Dehydrogenase†

Parvinder Hothi,‡ Jaswir Basran,‡ Michael J. Sutcliffe,‡,§ and Nigel S. Scrutton*,‡

Departments of Biochemistry and Chemistry, University of Leicester, University Road, Leicester LE1 7RH, United Kingdom

Received December 2, 2002; Revised Manuscript Received February 13, 2003

ABSTRACT: The reaction of PQQ-dependent methanol dehydrogenase (MDH) from *Methylophilus methylotrophus* has been studied by steady-state and stopped-flow kinetic methods, with particular reference to multiple ligand binding and the kinetic isotope effect (KIE) for PQQ reduction. Phenazine ethosulfate (PES; an artificial electron acceptor) and cyanide (a suppressant of endogenous activity), but not ammonium (an activator of MDH), compete for binding at the catalytic methanol-binding site. Cyanide does not activate turnover in *M. methylotrophus* MDH, as reported previously for the *Paracoccus denitrificans* enzyme. Activity is dependent on activation by ammonium but is inhibited at high ammonium concentrations. PES and methanol also influence the stimulatory and inhibitory effects of ammonium through competitive binding. Reaction profiles as a function of ammonium and PES concentration differ between methanol and deuterated methanol, owing to force constant effects on the binding of methanol to the stimulatory and inhibitory ammonium binding sites. Differential binding gives rise to unusual KIEs for PQQ reduction as a function of ammonium and PES concentration. The observed KIEs at different ligand concentrations are independent of temperature, consistent with their origin in differential binding affinities of protiated and deuterated substrate at the ammonium binding sites. Stopped-flow studies indicate that enzyme oxidation is not rate-limiting at low ammonium concentrations (<4 mM) during steady-state turnover. At higher ammonium concentrations (>20 mM), the low effective concentration of PES in the active site owing to the competitive binding of ammonium lowers the second-order rate constant for enzyme oxidation, and the oxidative half-reaction becomes more rate limiting. A sequential stopped-flow method is reported that has enabled, for the first time, a detailed study of the reductive half-reaction of MDH and comparison with steady-state data. The limiting rate of PQQ reduction (0.48 s^{-1}) is less than the steady-state turnover number, and the observed KIE in stopped-flow studies is unity. Although catalytically active, we propose reduction of the oxidized enzyme generated in stopped-flow analyses is gated by conformational change or ligand exchange. Slow recovery from this trapped state on mixing with methanol accounts for the slow reduction of PQQ and a KIE of 1. This study emphasizes the need for caution in using inflated KIEs, and the temperature dependence of KIEs, as a probe for hydrogen tunneling.

Methanol dehydrogenase (MDH; EC 1.1.99.8)[1] is a 2,7,9-tricarboxypyrroloquinoline quinone (PQQ)-dependent enzyme (*1*). MDH catalyses the oxidation of methanol to formaldehyde and utilizes a specific cytochrome *c* as electron acceptor (*2*). MDH from *Methylophilus methylotrophus* (W_3A_1) and *Methylobacterium extorquens* is known to adopt a $\alpha_2\beta_2$ structure (*3*−*5*). A calcium ion is coordinated to PQQ in each α subunit and operates as a Lewis acid during substrate oxidation. Hydride transfer and addition−elimination mechanisms have been proposed for methanol oxidation by MDH (*6*). Computational and high-resolution crystallographic studies favor a hydride transfer mechanism (*7*), which was also proposed for PQQ-dependent glucose dehydrogenase (*8*).

Methanol oxidation by MDH is assayed by reduction of phenazine ethosulfate (PES) and 2,6-dichlorophenol indophenol (DCPIP) (*9*). Ammonium salts are required for activity (*9*) but are also inhibitory at high concentration (*10*). Dye reduction (so-called endogenous activity) is observed in the absence of added substrate owing to the presence of contaminating alcohols and aldehydes in laboratory reagents and the broad specificity of MDH (*11*−*13*). Dealkylation of PES, especially at high pH, leads to aldehyde production and contributes further to endogenous activity (*14*). Endogenous activity is suppressed by cyanide, a competitive inhibitor with respect to substrate. Inactivation of MDH has been reported as a result of endogenous activity in the absence of added methanol, but this only occurs in the

† This work was funded by the Biotechnology and Biological Sciences Research Council, the Wellcome Trust, and the Lister Institute of Preventive Medicine. N.S.S. is a Lister Institute Research Professor.

* Corresponding author. Telephone: +44 116 223 1337. Fax: +44 116 252 3369. E-mail: nss4@le.ac.uk.

‡ Department of Biochemistry.

§ Department of Chemistry.

[1] Abbreviations: MDH, methanol dehydrogenase; PQQ, 2,7,9-tricarboxypyrroloquinoline quinone; TTQ, tryptophan tryptophylquinone; TPQ, topa quinone; PES, phenazine ethosulfate; DCPIP, dichlorophenol indophenol; QM/MM, quantum mechanical/molecular mechanical; KIE, kinetic isotope effect.

10.1021/bi027282v CCC: $25.00
Published on Web 03/11/2003

absence of cyanide (*13*). The main features of the reaction cycle have emerged from kinetic studies using artificial electron acceptors (*13*, *15*) and extended to studies with the physiological acceptor cytochrome c_L for *Hyphomicrobium X* and *Paracoccus denitrificans* MDH, respectively (*10*, *16*).

TPQ- and TTQ-dependent quinoproteins have become important model systems for studies of enzymatic hydrogen tunneling (*17*−*19*), but evidence for H-tunneling in PQQ-dependent enzymes is lacking. H-tunneling in enzymes at physiological temperatures has been inferred from the effects of atomic mass of the hydrogen nucleus on reaction rates by isotopic substitution (*20*), through studies of kinetic isotope effects (KIEs). Recent evidence supports mechanisms of H-transfer assisted by thermally induced fluctuations in protein structure in a small but growing number of enzymes, including quinoproteins (*17*, *18*), flavoproteins (*21*−*23*), alcohol dehydrogenases (*24*, *25*), and monooxygenases (*26*, *27*), and this questions the indiscriminate assumption that enzyme reactions proceed by classical over-the-barrier processes (for recent reviews see refs *28*−*31*). Experimental studies with tryptophan tryptophylquinone (TTQ)-dependent amine dehydrogenases indicate that proton transfer occurs by pure tunneling (i.e., from the ground state of the C−H bond vibration in the enzyme−substrate complex) during the breakage of a substrate C−H bond (*17*, *18*), consistent with theoretical models of H-tunneling (*32*, *33*) and hybrid quantum mechanical and molecular mechanical (QM/MM) computational studies (*34*, *35*). The measurement of KIEs in steady-state (e.g., *36*, *37*) and single turnover studies (e.g., *17*, *18*) has been used to investigate H-transfer by tunneling. In these studies, a detailed understanding of the origin of KIEs observed in kinetic studies is a prerequisite to any analysis of the mechanism of H-transfer. With this in mind, we have now extended our studies of H-transfer in quinoproteins to the PQQ-dependent MDH from *M. methylotrophus* (sp. W_3A_1), for which a crystallographic structure exists (*4*, *5*), to address the origin of the unusual kinetic isotope effects observed in steady-state reactions. We report the first detailed stopped-flow studies of PQQ reduction and oxidation by methanol and PES, respectively. We have also analyzed KIEs for methanol oxidation; established relationships with ammonium, PES, and cyanide concentration; and demonstrated temperature independent values for the KIE. Our work establishes that the unusual trend in KIE has its origin in the differential binding affinity of MDH for methanol and deuterated methanol and also in competitive binding of methanol or deuterated methanol to binding sites for ammonium and PES.

EXPERIMENTAL PROCEDURES

Materials. CHES (2-[*N*-cyclohexylamino]ethanesulfonic acid), MES (2-[*N*-morpholino]ethanesulfonic acid), DCPIP (2,6-dichlorophenol indophenol; sodium salt), PES (phenazine ethosulfate; *N*-ethyldibenzopyrazine ethyl sulfate salt), and potassium cyanide were obtained from Sigma. Ammonium sulfate and methanol were from Fisher chemicals. Deuterated methanol (methyl-d_3 alcohol-*d*, 99.8%) was from Aldrich. The chemical purity of the deuterated methanol was determined to be >99% by high-performance liquid chromatography, NMR, and gas chromatography, by the suppliers. Ferricenium hexafluorophosphate was synthesized as described (*38*).

Purification of MDH. M. methylotrophus (sp. W_3A_1) was grown aerobically at 30 °C on 0.5% (v/v) methanol, in three flasks containing 1 L each of mineral salts medium as described (*9*). Flasks were inoculated and cultured on a rotary shaker (220 rpm) at 30 °C for 2−3 days and used to inoculate a further 60 L of sterilized medium. Cultures were grown under vigorous aeration, at laboratory temperature. Cells were harvested in the late exponential phase, washed, and resuspended in 10 mM potassium phosphate buffer, pH 7.0. Owing to the labile nature of MDH, methanol (25 mM) was added before cell disruption and included in all buffers throughout purification (*39*). Cells were broken by passage through a French pressure cell (14 000 psi, 4 °C). DNA was hydrolyzed (DNase I), and cell debris was removed by centrifugation. The supernatant was applied to a DE-52 cellulose column equilibrated with 10 mM potassium phosphate buffer, pH 7.0. MDH was eluted with the same buffer and then applied to a hydroxyapatite column equilibrated with 10 mM potassium phosphate buffer, pH 7.0. Impurities were removed by washing with 0.2 M potassium phosphate buffer, pH 7.0; enzyme was eluted with 0.4 M potassium phosphate buffer, pH 7.0. Fractions containing MDH were dialyzed exhaustively against 25 mM MES buffer, pH 5.5 and applied to a CM-52 cellulose column equilibrated with the same buffer. Enzyme was eluted using a salt gradient (0−0.5 M NaCl contained in 25 mM MES buffer, pH 5.5). The peak of enzyme activity was eluted between 0.2 and 0.25 M NaCl. Active fractions were pooled and concentrated by ultrafiltration. Purified enzyme was stored at −80 °C in 25 mM MES buffer containing 25 mM methanol (pH 5.5). Enzyme was judged to be pure by SDS−polyacrylamide gel electrophoresis and the ratio of absorbance (11.3) at 280 and 345 nm (*39*). MDH was purified in the semiquinone form ($\epsilon_{343} = 28\,300\ M^{-1}\ cm^{-1}$ (*15*)). Prior to use in kinetic studies, the methanol added for storage was removed, and MDH was stabilized by exhaustive dialysis against 25 mM MES buffer, pH 5.5 containing 6 mM KCN, at 4 °C.

Steady-State Kinetic Analysis. Steady-state kinetic measurements were performed with a 1-cm light path in 0.1 M CHES buffer, pH 9.0, at 25 °C (unless stated otherwise) in a total volume of 1 mL. MDH activity was measured using a dye-linked assay in which the reduction of PES is monitored by coupling its oxidation to the reduction of DCPIP. Reduction of DCPIP was followed at 600 nm using a Perkin-Elmer Lambda 5 UV/vis spectrophotometer. The reaction mixture contained cyanide (6 mM; to suppress endogenous enzyme activity in the absence of added methanol), PES (1 mM), and DCPIP (0.04 mM). Ammonium sulfate (0.1−200 mM) and methanol (or deuterated methanol) were added to the reaction mix at the appropriate concentration (see Results). Enzyme concentration was typically 20 nM. PES was protected from light to prevent accumulation of formaldehyde, which is a substrate of MDH. Initial rates of reaction were monitored over 1−5 min (depending upon substrate concentration, activator concentration, and temperature). Initial velocity was expressed as μmol of product formed per μmol of enzyme per second using a molar absorption coefficient at 600 nm of 22 000 $M^{-1}\ cm^{-1}$ for DCPIP (*40*). Initial velocity data as a function of methanol concentration were analyzed by fitting to the standard Michaelis−Menten rate equation. Initial velocity data collected as a function of ammonium ion

concentration (L) were fitted to

$$v = \frac{\left(1 + \frac{b[L]}{K_i}\right)V_{max}}{1 + \frac{K_S}{[L]} + \frac{K_S}{K_i} + \frac{[L]}{K_i}} \quad (1)$$

where K_S and K_i are the activation and inhibition constants for ammonium, respectively. V_{max} is the theoretical maximum rate, and b is a factor by which the V_{max} is adjusted owing to inhibition. The use of eq 1 in studies of methanol dehydrogenase has been described (*10*).

Stopped-Flow Kinetic Studies of the Oxidative Half-Reaction. Stopped-flow studies were performed under anaerobic conditions since it has been suggested that molecular oxygen might compete with PES as an electron acceptor of PQQ in *Paracoccus* MDH (*41*). Anaerobic rapid kinetic experiments were performed using an Applied Photophysics SX.18MV stopped-flow spectrophotometer housed in a Belle Technology anaerobic glovebox (<5 ppm oxygen). Solutions used were made anaerobic by bubbling with argon for 2 h and left to equilibrate overnight in the glovebox. Studies of the oxidative half-reaction of MDH were performed by rapid mixing of MDH (4 μM), KCN (6 mM), and various concentrations of ammonium sulfate (see Results) in 0.1 M CHES buffer, pH 9.0, with various concentrations of PES at 5, 25, and 41 °C. The absorbance change, representing oxidation of the enzyme, was followed at 354 nm (isosbestic point of PES). Data were analyzed by nonlinear least squares regression analysis on an Acorn RISC PC using Spectrakinetics software (Applied Photophysics). For each reaction, at least three replicate measurements were collected and averaged, each containing 1000 data points. The absorbance change monitored was monophasic, and observed rates were obtained by fitting to a standard single-exponential expression.

Production of Oxidized Methanol Dehydrogenase and Sequential Stopped-Flow Studies of Enzyme Reduction. Oxidized MDH was generated transiently by rapid mixing of MDH in the stopped-flow instrument with the one electron acceptor ferricenium hexafluorophosphate under anaerobic conditions. MDH (4 μM) contained in 0.1 M CHES buffer, pH 9.0, 4 mM ammonium sulfate, and 6 mM KCN was mixed with an excess of ferricenium (32 μM). Complete oxidation occurred over approximately 10 s, after which the enzyme was reduced with 10 mM methanol using a sequential mixing protocol. Spectral changes were monitored using a photodiode array detector, and data were analyzed globally using ProKin software (Applied Photophysics) to identify intermediates. The dependence of the rate of enzyme reduction by substrate was performed using the same sequential mixing method. Enzyme reduction was followed at 342 nm, which is the wavelength corresponding to the major absorption peak of the two electron reduced form of MDH. Reaction transients were analyzed by fitting to a single-exponential expression.

RESULTS

Endogenous Activity and Effect of Cyanide in Steady-State Reactions. Cyanide is known to suppress endogenous activity in MDH isolated from *Paracoccus denitrificans* (*10*) and *Hyphomicrobium X* (*13*). Prior to embarking on a detailed steady-state characterization of MDH from *M. methylotrophus*, we investigated the optimal concentration of cyanide required to suppress endogenous activity. Complete suppression of endogenous activity was observed at cyanide concentrations of 6 mM (Figure 1) in assays using 20 mM ammonium sulfate and 1 mM PES. The presence of cyanide has little effect on initial velocities measured in the presence of saturating methanol and deuterated methanol (Figure 1). The lack of activation of methanol dependent activity by cyanide contrasts with observations made using MDH from *P. denitrificans*, where activation of activity was seen in the presence of cyanide (*10*). At low PES concentrations (100 μM) and low ammonium concentrations (4 mM), a cyanide concentration of 6 mM was also found to be sufficient to suppress the endogenous activity (data not shown).

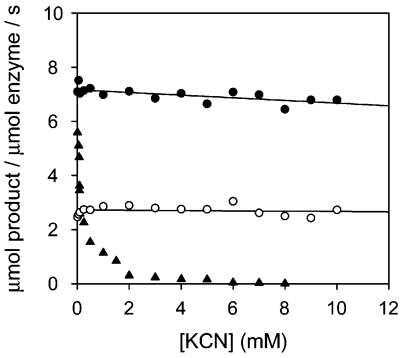

FIGURE 1: Plots of initial velocity vs cyanide concentration for endogenous and methanol dependent activity of MDH. Assays were performed at 25 °C as described in Experimental Procedures. Filled triangles, endogenous activity; filled circles, methanol dependent activity; and open circles, deuterated methanol dependent activity. Methanol and deuterated methanol concentration, 10 mM. Ammonium concentration, 20 mM; and PES concentration, 1 mM.

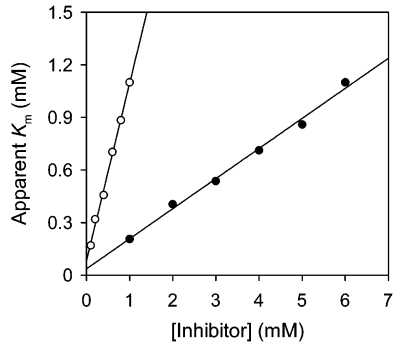

FIGURE 2: Plots of apparent K_m for methanol vs PES and cyanide concentration. Apparent Michaelis constants were determined by fitting initial velocity data to the Michaelis−Menten equation. Filled circles, apparent K_m as a function of KCN concentration. Conditions: ammonium, 4 mM; PES, 1 mM; and MDH, 20 nM. The apparent inhibition constant for KCN, K_i, is 211 ± 150 μM. Open circles, apparent K_m as a function of PES concentration. Conditions: ammonium, 4 mM; cyanide, 6 mM; and MDH, 20 nM. The apparent inhibition constant for PES, K_i, is 81 ± 19 μM.

Competitive Binding of PES and Cyanide to the Catalytic Methanol-Binding Site. Evidence for competitive binding of ligands to the catalytic methanol-binding site is shown in Figure 2. In steady-state reactions where the cyanide and ammonium concentrations are held constant at 6 and 4 mM, respectively, the apparent K_m for methanol increases with PES concentration (Figure 2). The apparent K_m for methanol

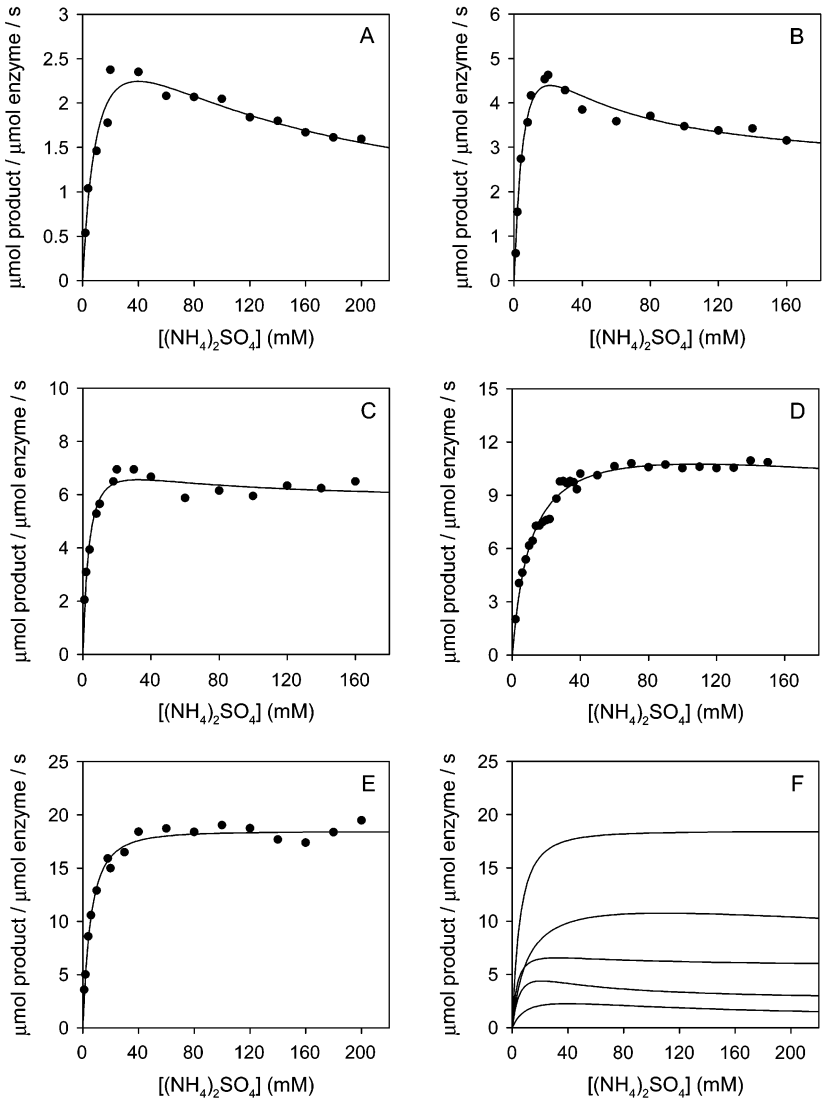

FIGURE 3: Plots of initial velocity vs ammonium concentration at different temperatures for the reaction catalyzed by MDH. Panels A−E, assays performed at 5, 10, 20, 30, and 40 °C. The fits shown are those to eq 1. K_s values (mM) at each temperature are 12.7 ± 5.1, 11.7 ± 1.7, 4.2 ± 1.5, 11.3 ± 2.0, and 8.5 ± 1.1 for panels A−E, respectively. Fitting to eq 1 produces K_i values (mM) with large associated errors owing to the limited ammonium concentration range. At 5 °C, K_i is 122.7 ± 62.5 mM, and this value increases substantially with increasing temperature. Panel F, composite illustrating the best fit line at all temperatures shown in panels A−E. Conditions: 0.1 M CHES buffer, pH 9.0, 10 mM methanol, 1 mM PES.

is also dependent on cyanide concentration in reactions where the ammonium concentration was fixed at 4 mM and the PES concentration was fixed at 1 mM (Figure 2). Combined, these data indicate that methanol, PES, and cyanide interact at the same or overlapping sites in MDH. Ammonium, however, does not compete at the catalytic methanol-binding site since the apparent K_m for methanol is not affected by ammonium concentration (range of 4−150 mM) at 1 mM PES (apparent K_m for methanol ∼1 mM) or 100 μM PES (apparent K_m for methanol ∼150 μM).

Initial Velocity Profiles as a Function of Ammonium Concentration and Temperature. A generally accepted model for the reaction cycle of MDH is that proposed by Frank et al. (*15*) and modified by Harris and Davidson to account for the inhibitory role of ammonium ions at high concentrations (*10*). To gain further insight into the effect of the activator during steady-state turnover, the effect of temperature (5−40 °C) and ammonium sulfate concentration (0.5−200 mM) was investigated. The methanol concentration was 10 mM (apparent K_m ∼1 mM at each temperature), and PES concentration was 1 mM. Initial velocity is stimulated at low concentrations of ammonium sulfate, whereas higher concentrations partially inhibit enzyme activity (Figure 3). Inhibition is reduced as temperature is increased (Figure 3). Fitting to eq 1 reveals that ammonium binding to the stimulatory site is essentially independent of temperature.

The inhibition response at different temperatures in the presence of high ammonium sulfate concentrations (>20 mM) highlights complications that arise in studies of methanol oxidation by MDH. However, these complications are less apparent at low ammonium concentrations (<4 mM) since the K_i value (>100 mM) is much greater than the ammonium concentration, and the K_s value (∼10 mM) is essentially constant over the temperature range of 5−40 °C. Enzyme activity is stable over a 24 h period and is unaffected by KCl concentration (range of 0−200 mM). This confirms that loss of enzyme activity at high ammonium concentrations is not attributable to stability or ionic strength effects.

Effect of Deuterated Methanol on Initial Velocity Profiles and Kinetic Isotope Effects. Reactions with deuterated

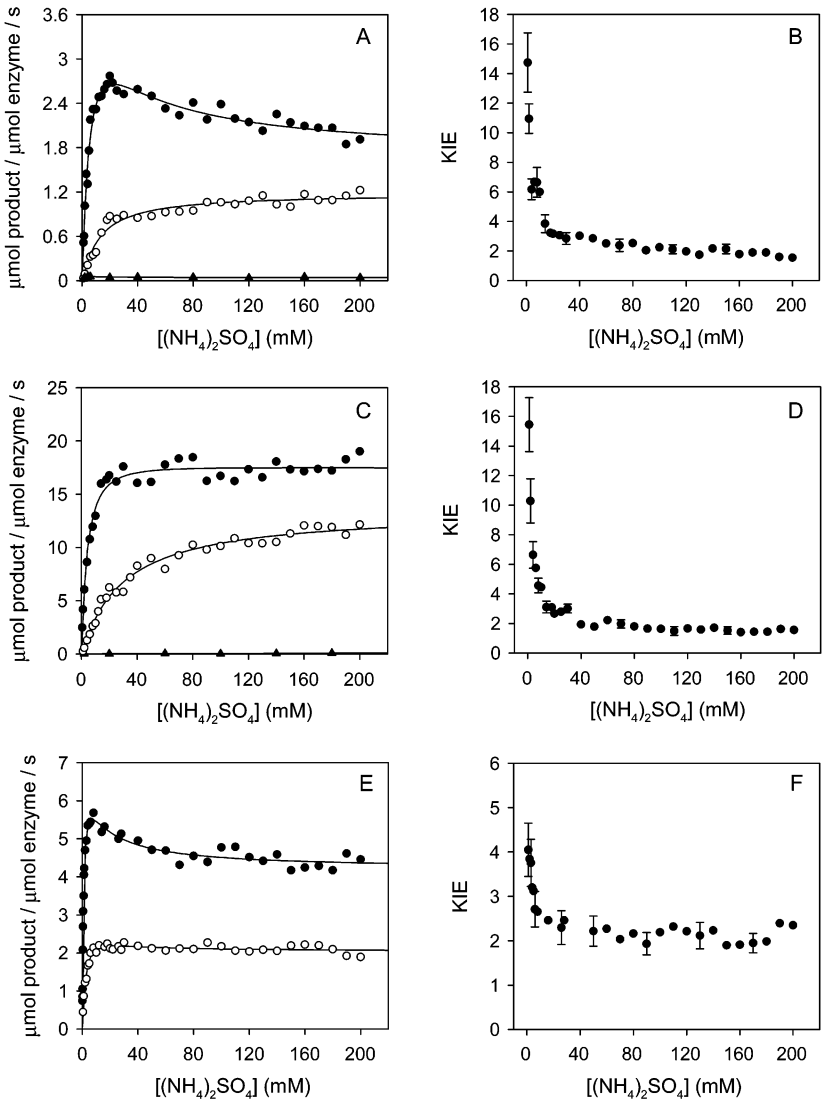

FIGURE 4: Plots of initial velocity with methanol and deuterated methanol vs ammonium concentration and variation in the observed kinetic isotope effect with ammonium concentration. Panel A, initial velocity vs ammonium concentration at 5 °C. Conditions: as for Figure 3. Filled circles, protiated methanol; open circles, deuterated methanol. Panel B, variation in KIE with ammonium concentration generated from the data shown in panel A. Panels C and D, as for panels A and B, respectively, but at 41 °C. Endogenous rates (i.e., in the absence of added substrate) are shown by filled triangles. Panels E and F, as for panels A and B, respectively, but with 200 μM PES at 25 °C. Filled circles, methanol; open circles, deuterated methanol. In panels A, C, and E each data point is the average of at least three independent measurements. The errors for each data point are propagated into panels B, D, and F, respectively, in the calculation of KIEs as a function of ammonium concentration (for clarity, not all error bars are shown).

methanol revealed a different trend in the dependence of initial velocity on ammonium concentration (Figure 4A,C). Unlike with methanol, the profile with deuterated substrate shows very weak inhibition at high ammonium concentration at 5 and 41 °C. The altered initial velocity profile explains the unusual relationship between ammonium concentration and the KIE (Figure 4B,D), observed also for *Methylobacterium extorquens* MDH (*42*). The KIE for *M. methylotrophus* MDH approaches 16 at low ammonium concentration and decreases with increasing ammonium concentration to approximately 1.5. The value of K_s (~25 mM) with deuterated methanol is slightly higher than with protiated substrate, suggesting weaker binding of ammonium to the K_s site with deuterated substrate. Deuteration of methanol clearly perturbs the initial velocity profiles, and the small force constant effects on methanol binding support the view that methanol competes with ammonium at the K_s and K_i binding sites.

We have also demonstrated that PES and ammonium compete for the K_s site seen in the dependence of initial velocity on ammonium sulfate concentration. Analysis of the initial velocity versus ammonium sulfate concentration at 200 μM PES (Figure 4E) indicates that the K_s value is smaller as compared to assays performed with 1 mM PES (Figure 4A,C). Moreover, with 200 μM PES, the effect of deuterated substrate on the K_s value is clearly seen, thus confirming that deuterated substrate binds less tightly to the K_s site (K_s values 1.0 ± 0.2 mM and 3.6 ± 0.9 mM with methanol and deuterated methanol, respectively; Figure 4E). Steady-state assays performed with 6 and 20 mM cyanide indicate that cyanide does not affect ammonium binding at the K_s and K_i sites (data not shown).

Temperature Dependence of Kinetic Parameters and Kinetic Isotope Effects at Fixed Ammonium Concentration. Steady-state reactions with protiated and deuterated methanol

Table 1: Kinetic Parameters Determined from Steady-State Reactions of MDH at Different Temperatures and Ammonium Ion Concentrations[a]

$[(NH_4)_2SO_4]$ (mM)	temp. (°C)	protiated methanol k_{cat} (s^{-1})	deuterated methanol k_{cat} (s^{-1})	protiated methanol K_m (mM)	deuterated methanol K_m (mM)
4	5	1.51 ± 0.04	0.36 ± 0.04	1.2 ± 0.14	1.2 ± 0.58
4	30	4.91 ± 0.12	0.99 ± 0.05	0.93 ± 0.09	1.1 ± 0.27
4	40	7.7 ± 0.19	1.23 ± 0.09	1.1 ± 0.12	1.1 ± 0.38
20	5	2.53 ± 0.06	1.11 ± 0.06	1.2 ± 0.11	1.4 ± 0.3
20	40	17.44 ± 0.57	7.41 ± 0.18	1.1 ± 0.15	1.1 ± 0.12
150	5	1.97 ± 0.06	1.12 ± 0.04	1.0 ± 0.13	1.5 ± 0.2
150	40	18.65 ± 0.6	8.01 ± 0.26	1.4 ± 0.17	1.5 ± 0.2

[a] Parameters were obtained by least-squares fitting of data to the standard Michaelis−Menten expression.

were investigated over the temperature range of 5−40 °C, at fixed ammonium concentrations. Plots of initial velocity versus methanol concentration were hyperbolic, and kinetic constants were obtained by fitting to the Michaelis−Menten expression (Table 1). The results show the expected increase in k_{cat} as ammonium concentration and temperature are increased. The apparent Michaelis constants for methanol and deuterated methanol are similar and are unaffected by ammonium concentration and temperature.

The temperature dependence of the observed KIE was investigated at 1, 4, and 20 mM ammonium sulfate, with saturating concentrations of methanol and deuterated methanol (80 mM). Eyring plots indicate that the KIE is independent of temperature (Figure 5), although reaction rates are strongly dependent on temperature. The parameters $\Delta H^{\ddagger}$ and A'^{H}:A'^{D} were obtained by fitting to eq 2 (Table 2).

$$\ln(k/T) = \ln k_B/h + \Delta S^{\ddagger}/R - \Delta H^{\ddagger}/RT \qquad (2)$$

The definitions of the terms A'^{H} and A'^{D} are given in our previous work (*17*). The temperature independence of the KIEs at each ammonium concentration is consistent with the value of the ratio A'^{H}:A'^{D} ~KIE > 1 and $\Delta\Delta H^{\ddagger}$ ~0 (Table 2). In these temperature dependence studies, only a fraction of the total enzyme population (9 and 30%, respectively) is bound to activator at 1 and 4 mM ammonium, but in the absence of ammonium MDH is not active. The presence of free MDH does not therefore complicate the analysis. Also, the K_s term is constant over the temperature range thus ensuring that the same fraction of enzyme remains bound to ammonium at each assay condition shown in Figure 5. We explored an alternative approach to the temperature dependence studies shown in Figure 5, which involved measuring initial steady-state velocities at different ammonium concentrations and temperatures and data fitting using eq 1 to obtain the true k_{cat} value (i.e., with full occupancy of the stimulatory ammonium site and zero occupancy of the inhibitory site). However, owing to the large number of variables in eq 1 it was not possible to determine the true k_{cat} values with adequate precision to assess with confidence the trend in KIE as a function of temperature.

Although temperature independent KIEs are observed with 20 mM ammonium (where there is maximal enzyme activity; Figure 3), the interpretation in this regime is potentially complicated by partial occupation of the inhibitory site by protiated methanol (particularly at low temperatures). The Eyring plots, however, are linear across the temperature range, suggesting that any inhibition is minor. The value of K_i is difficult to determine accurately owing to the limited ammonium concentration range used in Figure 3, but estimates >100 mM are not unreasonable. At 20 mM ammonium the inhibitory site would be ~15% occupied,

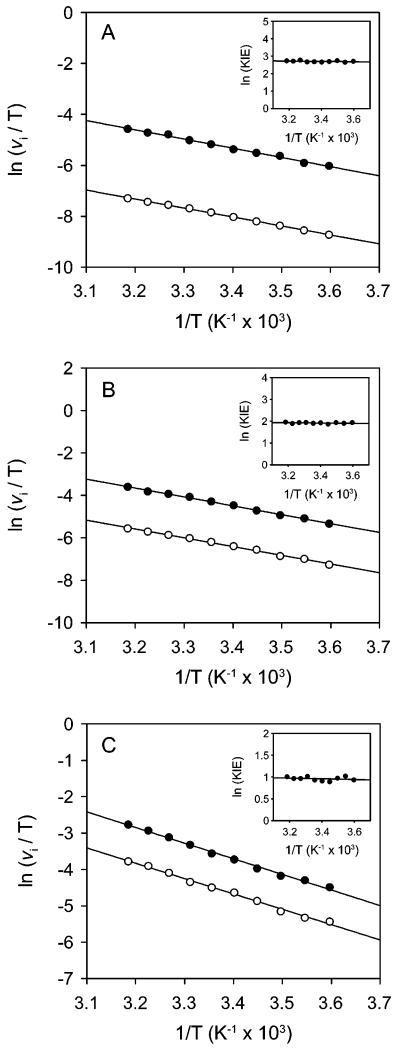

FIGURE 5: Eyring plots for steady-state reactions of MDH with methanol and deuterated methanol. Panel A, plot of ln v_i/T vs $1/T$ at 1 mM ammonium. Filled circles, protiated methanol; open circles, deuterated methanol. Inset, plot of ln KIE vs $1/T$. Enzyme concentration 20 nM for methanol and 240 nM for deuterated methanol. Panels B and C, as for panel A except with 4 and 20 mM ammonium, respectively. Conditions: as for Figure 3 except with 80 mM methanol or 80 mM deuterated methanol and enzyme concentration 20 nM. In these assays, one standard deviation in each activity measurement ($n = 7$) at a defined temperature and ammonium ion concentration is <6% of the determined value. Parameters derived from fitting of the data to the Eyring equation are given in Table 2.

Table 2: Kinetic and Thermodynamic Parameters Obtained from Fitting the Data Shown in Figure 5 to Eq 2

$[(NH_4)_2SO_4]$ (mM)	temp. range (°C)	$\Delta H^{\ddagger H}$ (kJ mol^{-1})	$\Delta H^{\ddagger D}$ (kJ mol^{-1})	A'^{H}: A'^{D}	KIE
1	5−41	30.0 ± 0.8	29.2 ± 0.4	20.6 ± 1.7	14.6 ± 1.9
4	5−41	34.9 ± 0.7	34.4 ± 0.7	8.4 ± 0.6	6.7 ± 0.7
20	5−41	35.7 ± 0.9	35.1 ± 1.0	3.4 ± 0.3	2.5 ± 0.2

assuming a K_i of 100 mM, and the K_s site would be ~67% occupied (K_s = 10 mM).

The data collected at 1 and 4 mM ammonium (Figure 5A,B) are essentially free of the complications that arise through partial occupation of the inhibitory site (see Figure 3). If PQQ reduction by methanol were fully rate-limiting (see below), the temperature independence of the KIE (~15 and ~7 at 1 and 4 mM ammonium, respectively) might be taken to suggest hydride transfer by a quantum tunneling mechanism from methanol to the PQQ cofactor in the enzyme−substrate complex. However, the evidence for tunneling is questionable owing to the complex effects of multiple ligand binding on the observed value of the KIE. The magnitude of the KIE is governed by the degree of occupation of the K_s site by ammonium. This in turn is influenced by the competitive binding of methanol and deuterated methanol at the same site, with deuterated methanol competing more effectively than protiated methanol. This leads to less stimulation of activity in steady-state reactions with deuterated methanol. The basis of the temperature independent kinetic isotope effects is thus difficult to resolve since one cannot readily separate the thermodynamic contributions arising from complex binding equilibria at the K_s site from those attributable to the chemical step (i.e., C−H/C−D bond cleavage). Further complex trends in the observed KIE were uncovered in studies of initial velocity and the KIE as a function of PES concentration. These studies are reported below.

Effect of PES Concentration on Initial Velocity Profiles and Kinetic Isotope Effects. The relationship between PES concentration (0.02−1 mM) and ammonium sulfate concentration (1, 2, 4, and 20 mM) was explored in steady-state assays in which the concentration of methanol and deuterated methanol was fixed at 10 mM. These analyses revealed that the observed KIE becomes larger as the electron acceptor concentration is increased (Figure 6A). A feature of the plot is that at low PES concentration the KIE approaches unity. Similar trends in KIE as a function of PES concentration were also observed at 5 and 41 °C (Figure 6B), and the KIE values at all PES concentrations were found to be independent of temperature (Figure 6B).

The relationship between ammonium sulfate and PES concentration on reaction rate can be observed more clearly when the initial velocity with protiated and deuterated methanol are plotted as a function of PES concentration (Figure 7A−D). As PES concentration increases, the initial velocity eventually becomes inhibited, but the extent of inhibition decreases at higher ammonium concentrations. The data suggest that ammonium and PES compete for a common binding site. Inhibition is more marked with deuterated methanol. Ammonium binding at the inhibitory site is less effective in the presence of deuterated methanol (Figure 4). This suggests that the more pronounced inhibition by PES

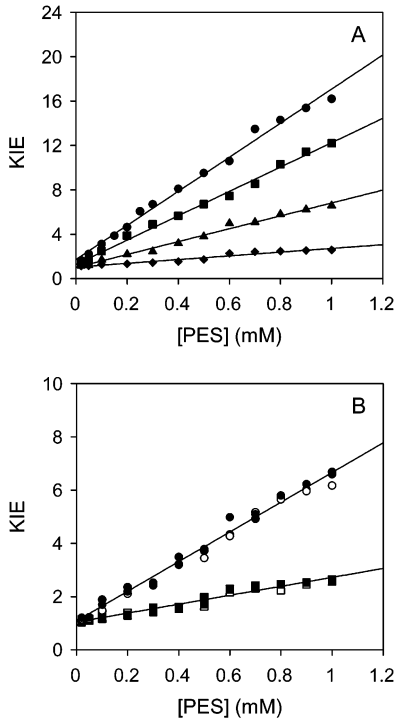

FIGURE 6: Dependence of the observed KIE value on ammonium sulfate and PES concentration. Panel A conditions: in 0.1 M CHES (pH 9.0), 25 °C, 10 mM methanol or deuterated methanol. Filled circles, filled squares, filled triangles, and filled diamonds represent ammonium sulfate concentrations of 1, 2, 4, and 20 mM, respectively. Panel B: Conditions as for panel A but temperature 5 °C (open symbols), 25 °C (gray symbols), and 41 °C (black symbols). Circles and squares represent assays performed in the presence of 4 and 20 mM ammonium sulfate, respectively.

with deuterated methanol (Figure 7A−D) is related to the weaker binding of ammonium at the same site. The weaker binding of ammonium to the inhibitory site in the presence of deuterated methanol results in an increase in the KIE since PES competes more effectively for the inhibitory site. Correspondingly, as ammonium concentration is increased, PES competes less effectively for the inhibitory site (Figure 7D). Similar trends to those shown in Figure 7 were also seen in assays performed at 5 and 41 °C (data not shown).

The complex binding equilibria at the K_s and K_i sites coupled with the differential binding affinities of methanol and deuterated methanol influences the degree of activation and inhibition of MDH. This competition gives rise to the unusual trends seen in the KIE values as a function of ammonium and PES concentration. At low PES concentrations the KIE approaches unity, and in this regime the KIE values are also potentially influenced by a change in the rate-limiting step since the rate of the oxidative half-reaction is expected to be second order with respect to PES concentration. With this additional complication in mind we describe below studies of the rate of the oxidative half-reaction of reduced MDH as a function of PES concentration.

Stopped-Flow Studies of the Oxidative Half-Reaction of MDH. Stopped-flow kinetic studies of electron transfer from semiquinone MDH to PES were performed under pseudo first-order conditions with respect to PES concentration. Reactions were monitored as a monophasic decrease in absorbance at 354 nm (an isosbestic point of PES), which represents the oxidation of MDH (Figure 8A). Kinetic studies

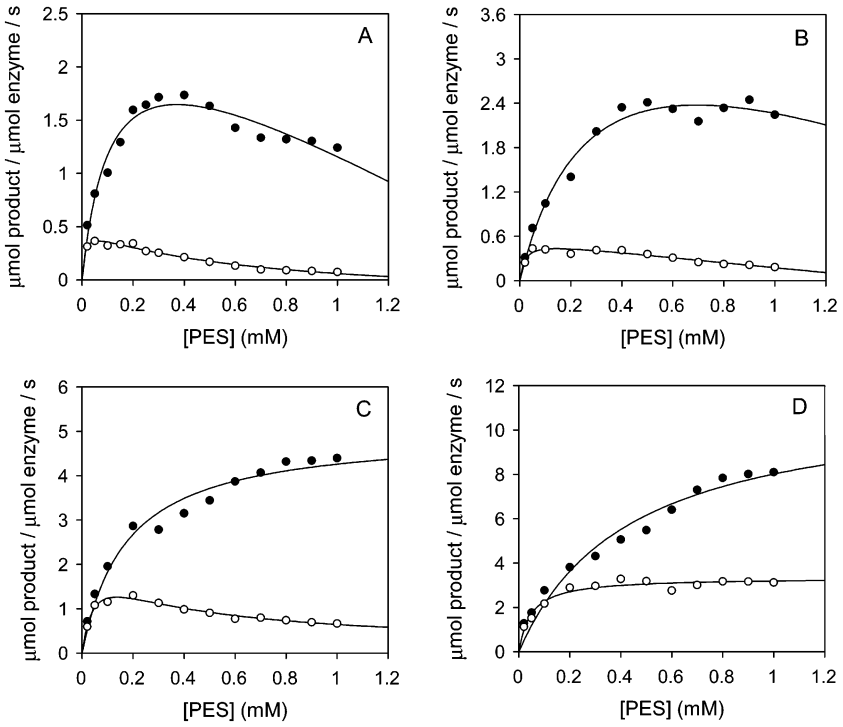

FIGURE 7: Initial velocities for protiated and deuterated methanol as a function of ammonium sulfate and PES concentration. Plots indicate reaction rates used to calculate the KIEs shown in Figure 6A. Conditions: as for Figure 6. Panels A−D: Reactions in the presence of 1, 2, 4, and 20 mM ammonium sulfate, respectively. Filled circles, protiated methanol; open circles, deuterated methanol each at 10 mM concentration.

were performed at 5, 25, and 41 °C. At each temperature, observed rates of electron transfer were second order with respect to PES concentration (Figure 8B), and the second-order rate constant for enzyme oxidation was found to depend on the ammonium sulfate concentration. This is attributable to the competitive binding of ammonium and PES in the active site of MDH, as inferred from our steady-state turnover experiments. Many binding sites for PES that are competent for electron transfer might exist in MDH. Our data reveal, however, that binding of PES to a site where methanol also binds makes a substantial contribution to the kinetics of electron transfer in MDH. These stopped-flow studies indicate, for the first time, that ammonium also controls the rate of the oxidative half-reaction in MDH, and the model for this regulation by ammonium is likely to be similar to the multiple ligand binding model advanced for the reductive half-reaction. Thus, at high ammonium concentrations, the effective concentration of PES in the electron transfer competent site of MDH is reduced, and the second-order rate constant for enzyme oxidation is correspondingly lowered. The converse situation would hold at low ammonium concentration, accounting for larger second-order rate constants for enzyme oxidation. Table 3 summarizes the rate constants for oxidation of MDH (extrapolated to 1 mM PES) at different ammonium concentrations and compares these values to the corresponding turnover numbers determined at 1 mM PES. In general, the rate of enzyme oxidation at 1 mM PES is faster than steady-state turnover measured at low ammonium concentrations, indicating that the reductive half-reaction is rate limiting. In this regime, the unusual dependence of the KIE value on ammonium (Figure 4) and PES (Figure 6) concentration is primarily determined by the complex binding equilibrium at the K_s and K_i sites. At high ammonium concentration the second-order rate constant for enzyme oxidation approaches k_{cat}; thus, the oxidative half-reaction is expected to contribute to rate limitation in steady-state turnover. In this regime, the KIE values are reduced but still show unusual dependencies on ligand and substrate concentrations, reflecting the competitive binding of PES, ammonium, and methanol to MDH, with concomitant effects on the kinetics of the reductive and oxidative half-reactions.

Single Turnover Studies of the Reductive Half-Reaction. Single turnover studies were pursued in the stopped-flow instrument to access the kinetics of the reductive half-reaction. MDH is purified in the semiquinone form. The oxidized form of MDH is highly labile, and this has prevented detailed analysis of the reductive half-reaction by other workers. The only report of an oxidized form of the enzyme is for MDH from *Hyphomicrobium* X (*15*), but detailed studies of the reductive half-reaction were not reported. Other workers have isolated oxidized forms of mutant MDH enzymes, which was possible owing to the reduced affinity of the enzyme for endogenous substrate (*42*, *43*).

We made initial attempts to oxidize MDH_{sq} using PES, immediately prior to a stopped-flow reaction in which methanol was mixed with enzyme. PES absorbs strongly in the region of interest (around the 342 nm region, which corresponds to the absorption peak for reduced MDH). Titration of PES with sodium dithionite identified a suitable isosbestic point at 354 nm, where changes in the redox state of MDH could be monitored without interference from PES (Figure 9, inset).

Single turnover experiments under anaerobic conditions involved the rapid mixing of 4 μM enzyme oxidized in the presence of 4 μM PES, 4 mM ammonium sulfate, and 6 mM

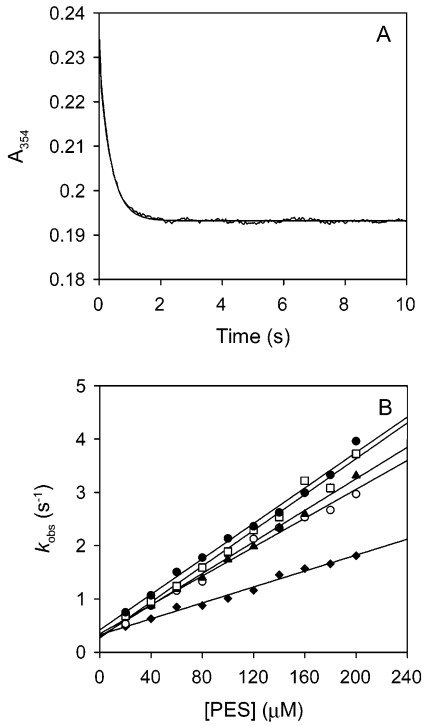

FIGURE 8: Plot of observed rate for the oxidative half-reaction of MDH as a function of PES concentration. Conditions: MDH_{sq} (4 μM), 0.1 M CHES, pH 9.0, 25 °C. Panel A: example of absorbance change monitored at 354 nm. The monophasic fit to the data is shown superimposed over the raw data. Panel B: filled circles, open squares, filled triangles, open circles, and filled diamonds represent reactions conducted in the presence of 0, 1, 2, 4, and 20 mM ammonium sulfate, respectively. Similar plots were constructed at 5 and 41 °C (not shown).

Table 3: Comparison of the Rate Constants[a] for the Oxidative Half-Reaction of MDH with the Turnover Number Determined from Steady-State Analysis

$[(NH_4)_2SO_4]$ (mM)	k_{obs} (s^{-1}) 5 °C	k_{cat} (s^{-1}) 5 °C	k_{obs} (s^{-1}) 25 °C	k_{cat} (s^{-1}) 25 °C	k_{obs} (s^{-1}) 41°C	k_{cat} (s^{-1}) 41 °C	KIE
0			17.06				
1	2.88	0.68	16.5	1.7	60.07	3.5	16
2			14	3.0			12
4	2.64	1.49	13.89	4.4	44.63	7.22	6.7
20	2.18	2.1	7.8	6.83	27.38	14.5	2.5

[a] Extrapolated to 1 mM PES.

KCN in 0.1 M CHES buffer, pH 9.0, with 10 mM methanol. Analysis of transients using a single-exponential expression for reactions performed with protiated and deuterated methanol yielded rate constants of 0.38 ± 0.01 and a KIE of 1 (Figure 9). A single mixing protocol was also used in which methanol and deuterated methanol were incubated with MDH prior to oxidation with PES, thus ensuring that the oxidized enzyme is stabilized by the presence of methanol. In this case, the reaction transient recorded the oxidation of the enzyme prior to enzyme reduction (data not shown). The rate of enzyme reduction and the KIE value were identical to those measured for MDH that had been oxidized in the absence of methanol. A KIE of 1 in single turnover stopped-flow studies of PQQ reduction was unexpected. However, oxidation of MDH by PES generated an oxidized MDH that occasionally could not be reduced by substrate, prompting concerns about the stability of the

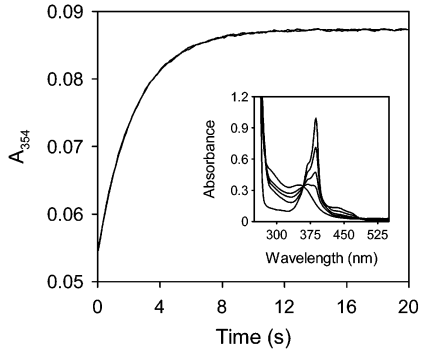

FIGURE 9: Stopped-flow reduction transient for oxidized MDH mixed with methanol and deuterated methanol. Conditions: 0.1 M CHES buffer, pH 9.0, 25 °C. Enzyme concentration 4 μM oxidized with 4 μM PES. Ammonium sulfate, 4 mM; cyanide, 6 mM. Substrate concentrations, 10 mM. Observed rate constant is 0.38 ± 0.01 s^{-1} for both substrates. Inset, titration of PES with dithionite showing the isosbestic point at 354 nm.

enzyme and leading us to explore alternative oxidants for MDH. Ferricenum hexafluorophosphate was found to be advantageous over PES as an oxidant of MDH since, unlike PES, it does not absorb strongly in the region of the PQQ chromophore. This feature allowed us to observe the full absorption peak of PQQ during enzyme reduction/oxidation and unlike with PES did not restrict our measurement of absorption changes for PQQ to an isosbestic point for the electron acceptor. PES also suffers from photodegradation that generates formaldehyde, a substrate of MDH, whereas the ferricenium ion is stable. Our work with PES demonstrated that the KIEs observed in steady-state reactions could not be reproduced in stopped-flow measurements (where the PES concentration is much lower than that in steady-state reactions), and it was important to establish if this is also a feature with other electron acceptors. In an improved stopped-flow method, we used a sequential mixing protocol in which MDH_{sq} was initially oxidized by mixing with ferricenium. In the second mix, and after a suitable delay time, methanol was introduced to the oxidized form of MDH. By using the sequential mixing procedure, the time elapsed (10 s) after generating oxidized enzyme and before reducing with methanol is substantially shortened, thus eliminating potential complications arising from the instability of oxidized MDH. Spectrum c (Figure 10) is very similar to that of oxidized MDH in which the active site calcium ion is replaced by barium (*42*).

Ferricenium was rapidly mixed with MDH contained in 0.1 M CHES buffer, pH 9.0 with 4 mM ammonium sulfate and 6 mM KCN, under anaerobic conditions. Photodiode array detection revealed that complete oxidation occurred within 10 s at 25 °C. Studies with various concentrations of ferricenium showed that oxidized MDH_{ox} was formed only when an excess of ferricenium was used (4 μM MDH:32 μM ferricenium). With stoichiometric ferricenium, formation of MDH_{ox} is incomplete owing to rereduction by endogenous activity. Spectral changes (Figure 10A) from oxidation reactions with a 4-fold excess of ferricenium were best described by a three step kinetic model A → B → C → D by global analysis with rate constants 9.7 ± 0.1 s^{-1} (A → B), 1.56 ± 0.01 s^{-1} (B → C), and 0.11 ± 0.005 s^{-1} (C → D). Spectrum a is the reduced enzyme, spectrum c oxidized enzyme, and spectrum b an intermediate that forms

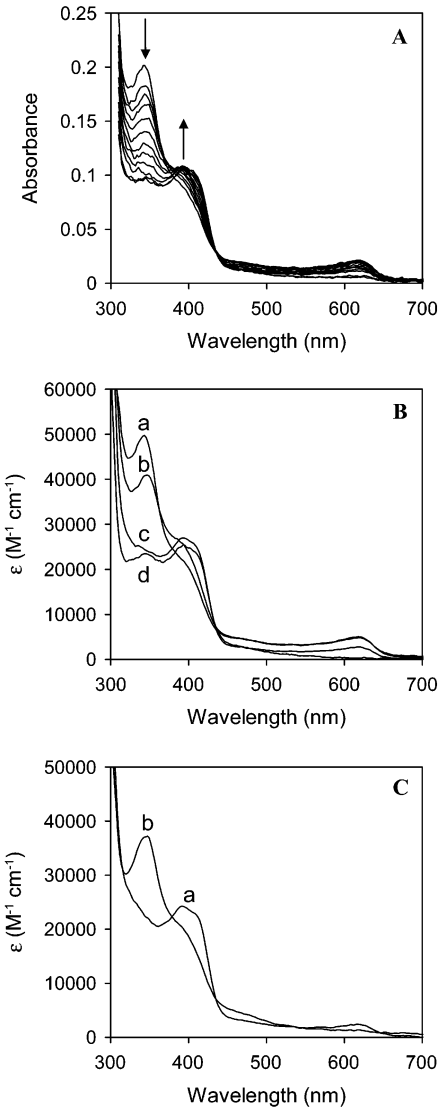

FIGURE 10: Oxidation of MDH by ferricenium hexafluorophosphate and reduction by methanol. Conditions: in 0.1 M CHES buffer, pH 9.0, 4 mM ammonium sulfate, 6 mM KCN, 4 μM MDH, 32 μM ferricenium, under anaerobic conditions at 25 °C. Panel A: Spectral changes accompanying enzyme oxidation. Panel B: Spectral intermediates identified by fitting to a 3-step kinetic model. There is a small contribution made by ferricenium to the absorption of MDH in the 340−400 nm region. Panel C: Reduction of oxidized MDH. Ferricenium (16 μM) was rapidly mixed with MDH (2 μM) and following a 10 s delay mixed with methanol (10 mM); all other conditions as in panel A. Spectrum a, oxidized enzyme; spectrum b, two electron reduced enzyme. Data were best fit to a one-step kinetic model with a rate constant of 0.36 ± 0.001 s^{-1}.

during enzyme oxidation, the identity of which is uncertain (Figure 10B).[2] Spectrum d shows a slight increase in absorbance at 342 nm (corresponding to the reduced peak of the enzyme), which suggests some reduction of the oxidized enzyme by endogenous activity. Ferricenium does not absorb significantly in the region of interest, and the

[2] The as-purified enzyme is often referred to as semiquinone MDH. However, it is likely that this form of the enzyme also contains some hydroquinone. Therefore, a number of species might form during the reoxidation of reduced MDH with a single electron acceptor such as the ferricenium ion. Species B might represent pure semiquinone MDH, following the oxidation of the small amount of hydroquinone present in species A.

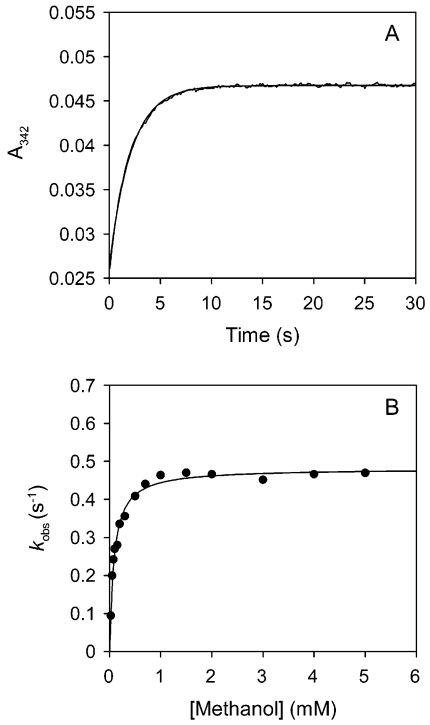

FIGURE 11: Reaction of oxidized MDH with protiated methanol. Conditions as in Figure 10C. Panel A: example of absorbance change monitored at 342 nm. Panel B: data fitted to the rapid equilibrium model of Strickland et al. (*44*).

deconvoluted spectra are thus attributed to the different redox states of MDH.

Following oxidation of MDH in the stopped-flow instrument, methanol (10 mM) was rapidly mixed with the enzyme solution to generate the two electron reduced spectrum of MDH (Figure 10C). The data confirm that the sequential mixing method generates oxidized MDH that is catalytically active. Rates of PQQ reduction are identical with protiated and deuterated methanol, consistent with the transients obtained with enzyme oxidized by PES. The molar absorption coefficient determined for oxidized MDH_{ox} is 24 170 M^{-1} cm^{-1} at 390 nm.

PQQ Reduction as a Function of Methanol Concentration. Using the sequential mixing method, reductive transients were collected as a function of methanol concentration in single wavelength absorption mode (342 nm). Absorption transients exhibited a monophasic increase in absorption corresponding to reduction of oxidized enzyme by methanol (Figure 11A). Data are shown in Figure 11B and were analyzed by fitting to the rapid equilibrium model of Strickland et al. (*44*), assuming no reverse reaction (as indicated by the lack of an ordinate intercept in the plot shown in Figure 11). The limiting rate of PQQ reduction is 0.48 ± 0.01 s^{-1}, and the apparent dissociation constant for the oxidized enzyme−methanol complex is 84 ± 6 μM. The limiting rate of PQQ reduction is less than the steady-state turnover number. The data suggest that enzyme reduction is not limited by hydride transfer (since KIE = 1). Although catalytically active, we propose reduction of the oxidized enzyme generated in stopped-flow analyses is gated by conformational change or ligand exchange. Slow recovery from this trapped state on mixing with methanol accounts for the slow reduction of PQQ and a KIE of 1. These data suggest, therefore, that the oxidized form of MDH generated

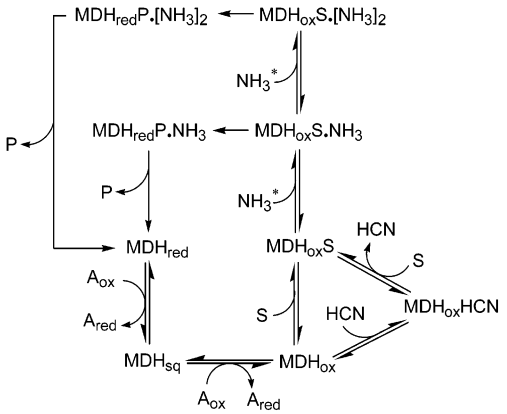

FIGURE 12: Proposed kinetic mechanism for the reaction cycle of MDH. A represents artificial electron acceptor; S and P represent substrate and product, respectively. The asterick indicates that the binding of ammonium is competitive with respect to the binding of the artificial electron acceptor and methanol. Two binding sites for ammonium are shown, corresponding to the K_s and K_i sites.The rate of enzyme reoxidation by electron transfer to the artificial electron acceptor, A, is also affected by competitive binding of ammonium to the electron acceptor site. Thus, the species MDH_{red} and MDH_{sq} represent different forms of reduced MDH representing a distribution of ammonium-bound and ammonium-free forms. For clarity, these different forms have been represented by single species for each oxidation state (i.e., MDH_{red} and MDH_{sq}).

in stopped-flow studies is different to that populated under multiple turnover conditions in the steady state.

DISCUSSION

It has been recognized for some time that ammonium ions modulate the activity of MDH in steady-state assays employing artificial electron acceptors. Frank et al. demonstrated that ammonium stimulates activity in steady-state assays with MDH from *Hyphomicrobium X* (*15*). Inhibition of activity at high ammonium concentrations was demonstrated later by Harris and Davidson (*10*), and these authors proposed a detailed kinetic mechanism for the reaction cycle of *P. denitrificans* MDH involving the stimulatory and inhibitory effects of ammonium and a role for cyanide in activation of MDH. Goodwin and Anthony identified an unusual dependence of KIE values on ammonium concentration, and they concluded that the reductive half-reaction is rate-limiting in steady-state turnover (*42*). The mechanistic basis for these unusual KIEs, however, was not elucidated. Given the complex nature of ligand binding in the active site of MDH we set out to elucidate the origin of this unusual dependence in *M. methylotrophus* MDH, for which a crystallographic structure is available (*4*), and to investigate if the value of the KIE is also influenced by factors other than the bond breakage reaction.

As a prerequisite to detailed studies of the KIE dependence on ligand and substrate concentration, we have shown that the steady-state behavior of *M. methylotrophus* MDH (Figure 12), despite some modifications, is in broad agreement with that of MDH isolated from other sources. The kinetic model incorporates two binding sites for ammonium (i.e., the K_s and K_i sites) identified from studies of initial velocity versus ammonium sulfate concentration (Figure 3), which gives rise to two catalytic routes to the two electron reduced form of MDH. Also, ammonium binding to the K_s and K_i sites is in competition with the binding of PES (Figures 6A and 7) and methanol (Figure 4), and this has major effects on the value of the KIE as a function of ammonium concentration (see below). Unlike with the *P. denitrificans* enzyme, we see no activation of turnover by cyanide (Figure 1). This apparent discrepancy between our work and that reported for the *P. denitrificans* MDH might arise from differences in data analysis. In studies with *P. denitrificans* MDH, the endogenous rate was subtracted from those measured in the presence of methanol to obtain a corrected rate for methanol turnover (*10*). Our studies with *M. methylotrophus* MDH indicate that subtraction is inappropriate (Figure 1) because at low cyanide concentrations the endogenous rate is greater than that observed with deuterated methanol. This indicates that the binding of methanol suppresses endogenous activity, which is consistent with the binding and oxidation of endogenous substrate and methanol at the same catalytic site. Our initial velocity studies have also indicated that PES and cyanide are competitive inhibitors at the catalytic site with respect to the binding of methanol to oxidized MDH (Figure 2). The competitive binding of cyanide at the catalytic site (lower triangular route in Figure 12) is consistent with cyanide suppressing endogenous activity—competitive binding will clearly prevent the binding of endogenous substrate at this site.

Our stopped-flow work of the oxidative half-reaction has additionally revealed for the first time that ammonium concentration also has a profound effect on the rate of enzyme reoxidation (Figure 8). This is attributed to competitive binding of ammonium and PES to a common, electron-transfer competent site in MDH. As ammonium concentration is increased, PES will be displaced from this site, and the effective concentration of PES will be lowered. Since electron transfer from reduced MDH to PES shows a second-order dependence on PES concentration (Figure 8), the effect of increasing ammonium concentration is to reduce the rate of enzyme oxidation. In the kinetic scheme for the MDH catalytic cycle (Figure 12) it is important to appreciate, therefore, that the reduced forms of MDH (i.e., MDH_{red} and MDH_{sq}) are not single species but represent a distribution of multiple forms of reduced enzyme in which ammonium is bound to, or absent from, the active site.

We have shown different binding affinities for protiated and deuterated methanol at the stimulatory (K_s) and inhibitory (K_i) ammonium binding sites (Figure 4). These differences are likely related to force constant effects for the C−H versus C−D bond. The shorter C−D bond results in a larger charge density and thus is electron supplying relative to C−H. Also, the perdeuterated substrate has a greater reduced mass for the CD_3O−H stretching vibration and therefore lies lower in the asymmetric potential energy well. We have observed similar force constant effects on the binding of methylamine and deuterated methylamine to TTQ-dependent methylamine dehydrogenase (*17*). The ability of deuterated methanol to compete more effectively than protiated methanol for the ammonium binding sites has obvious consequences for the degree of stimulation by ammonium and inhibition at high ammonium or high PES concentrations. Perturbation of these binding equilibria as a function of isotopic substitution (or PES concentration) will contribute to the observed KIE as we have demonstrated (Figures 4 and 6) because there is less stimulation of activity by ammonium with deuterated methanol. The possibility exists that the large KIE values

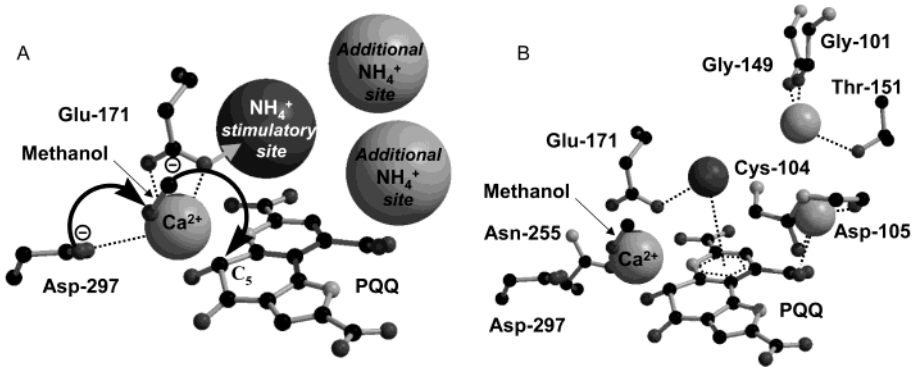

FIGURE 13: Active site of MDH. Panel A: the flow of electrons in the rate-determining step, predicted ammonium binding sites, and the proposed enhancement of Ca^{2+} as a Lewis acid by the stimulatory ammonium is illustrated. The modeling suggests the stimulatory site adjacent to Glu-171 and two additional sites, one or both of which could be inhibitory sites. Panel B: illustration of interactions with MDH (dashed lines) that could stabilize ammonium in the three suggested binding sites.

observed at low ammonium concentrations in steady-state turnover are, in the main, attributable to differential binding effects and that the true KIE associated with bond breakage is rather small (possibly ~2 as seen at high ammonium concentration). The temperature independence of the observed KIE seen at different ligand/substrate concentrations (Figure 5) is consistent with a mechanism in which competitive binding of the ligands and substrate at the stimulatory and inhibitory sites influences the KIE. Our analysis emphasizes the potential complications arising from multiple ligand binding to an enzyme active site. There is clearly a need to understand the mechanistic basis of observed KIEs in enzyme systems prior to using the temperature dependence of these values as probes of enzymatic H-tunneling. In the case of MDH, the relatively large KIEs seen in steady-state reactions at low ammonium concentration are attributed to differential binding effects of methanol and deuterated methanol at the K_s site, and competitive binding of PES and ammonium at this site modulates the value of the KIE. This is clearly seen in the kinetic response on altering the ammonium or PES concentration (Figure 4). At relatively high ammonium concentrations (>20 mM), the situation is more complex; in this regime, the KIE is also affected by the differential binding effects of methanol and deuterated methanol at the K_i site and the competition for binding by PES and ammonium (Figure 4). Additionally, however, the oxidative half-reaction makes a larger contribution to rate limitation owing to the competitive binding of PES and ammonium at the electron-transfer competent site (Figure 6; Table 3). Consequently, the KIE is deflated as compared with that observed at low ammonium concentration (Figure 4). We have attempted to develop stopped-flow methods to investigate the kinetics of PQQ reduction by methanol and deuterated methanol, thus enabling us to measure the intrinsic KIE for C—H/C—D bond cleavage. The labile nature of the oxidized form of MDH has prevented detailed study of the reductive half-reaction by other workers. Herein, we have developed a sequential stopped-flow method for transiently generating the oxidized form of MDH using ferricenium hexafluorophosphate as electron acceptor. Although this electron acceptor cannot be used in steady-state assays owing to adduct formation with cyanide, the kinetics of adduct formation are sufficiently slow to enable its use in single-turnover studies. Our stopped-flow studies have allowed us to measure for the first time the limiting rate of PQQ reduction (Figure 11B). However, this limiting rate (0.48 s^{-1}) is slower than the steady-state turnover number, and the lack of a KIE on PQQ reduction (Figure 11A; data for protiated and deuterated methanol are identical) indicates that bond cleavage is not rate limiting. Clearly, further studies are required to identify the nature of the gating step for PQQ reduction, and we are currently pursuing this line of inquiry.

The locations of the K_i and K_s sites for ammonium, methanol, and PES have not been defined in structural terms. However, spectral perturbation of MDH on addition of ammonium sulfate indicates binding close to the PQQ cofactor (*10*). We have used computational approaches to suggest the location of these ammonium sites. Analyzing the active site of MDH (*7*) with an ammonium-like probe (with the program GRID (*45*)) predicts ammonium forms a salt bridge (Figure 13A) with Glu-171 (this site is occupied in the crystal structure by water-97). The second carboxyl oxygen of Glu-171 coordinates the Ca^{2+}, which acts as a Lewis acid in the hydride transfer mechanism (*7*). Thus, the ammonium might be positioned to withdraw negative charge from Glu-171, resulting in the Ca^{2+} becoming more positive. This might allow the Ca^{2+} to function more effectively as a Lewis acid, thereby accelerating PQQ reduction by methanol. This electrostatic enhancement of activity provides an attractive model for stimulation of activity by ammonium. Other workers have observed iminoquinone formation between PQQ trimethylester and ammonia in organic solvents (*46*) and the spectral changes accompanying this reaction are similar to those observed on titrating *P. denitrificans* MDH with ammonium sulfate (*10*). Although stimulation of activity through the formation of an iminoquinone cannot be ruled out, perturbation of the electronic environment of PQQ by ammonium binding is, in our view, a more attractive proposition. Our modeling also gives possible insight into why, at higher concentrations, the stimulatory activity of ammonium is reduced. Two additional ammonium binding sites are identified within ~5 Å of the first (close to water-63 and water-65 in the crystal structure). Occupation of these sites could impair electrostatically at higher ammonium concentrations binding at the stimulatory site. Interactions that could stabilize ammonium in these three suggested binding sites are shown in Figure 13B. Like ammonium, PES is cationic and could occupy the same sites. Additionally, GRID suggests that a cationic molecule could compete directly for the methanol binding site. Our experimental

results show that PES, unlike ammonium, competes for binding at the catalytic methanol-binding site.

Our work has provided a mechanistic basis for the unusual KIEs observed in multiple turnover reactions of MDH, and it highlights complexities that arise in using artificial electron acceptors and ligands in studies with this enzyme. Our work also emphasizes the need for caution in using studies of the temperature dependence of KIEs, and inflated KIEs, as probes for H-tunneling. In the case of MDH, differential binding effects give rise to inflated KIEs at low ammonium concentrations and are likely to be responsible for the temperature independent KIEs observed at different ligand and electron acceptor concentrations. Kinetic studies with the physiological electron acceptor (a *c*-type cytochrome), which might not require stimulation with ammonium sulfate, are currently being pursued in attempts to obtain evidence for quantum mechanical tunneling reactions in MDH.

REFERENCES

1. Anthony, C. (2000) *Subcell. Biochem. 35*, 73−117.
2. Anthony, C. (1992) *Biochim. Biophys. Acta 1099*, 1−15.
3. Ghosh, M., Anthony, C., Harlos, K., Goodwin, M. G., and Blake, C. (1995) *Structure 3*, 177−187.
4. Xia, Z., Dai, W., Zhang, Y., White, S. A., Boyd, G. D., and Mathews, F. S. (1996) *J. Mol. Biol. 259*, 480−501.
5. Xia, Z. X., He, Y. N., Dai, W. W., White, S. A., Boyd, G. D., and Mathews, F. S. (1999) *Biochemistry 38*, 1214−1220.
6. Zheng, Y. J., and Bruice, T. C. (1997) *Proc. Natl. Acad. Sci. U.S.A. 94*, 11881−11886.
7. Zheng, Y. J., Xia, Z., Chen, Z., Mathews, F. S., and Bruice, T. C. (2001) *Proc. Natl. Acad. Sci. U.S.A. 98*, 432−434.
8. Oubrie, A., Rozeboom, H. J., Kalk, K. H., Olsthoorn, A. J., Duine, J. A., and Dijkstra, B. W. (1999) *EMBO J. 18*, 5187−5194.
9. Day, D. J., and Anthony, C. (1990) *Methods Enzymol. 188*, 210−216.
10. Harris, T. K., and Davidson, V. L. (1993) *Biochemistry 32*, 4362−4368.
11. Anthony, C., and Zatman, L. J. (1964) *Biochem. J. 92*, 614−621.
12. Duine, J. A., Frank, J., and Westerling, J. (1978) *Biochim. Biophys. Acta 524*, 277−287.
13. Duine, J., and Frank, J. (1980) *Biochem. J. 187*, 213−219.
14. Frank, J., and Duine, J. A. (1990) *Methods Enzymol. 188*, 202−209.
15. Frank, J., Dijkstra, M., Duine, J. A., and Balny, C. (1988) *Eur. J. Biochem. 174*, 331−338.
16. Dijkstra, M., Frank, J., and Duine, J. A. (1989) *Biochem. J. 257*, 87−94.
17. Basran, J., Sutcliffe, M. J., and Scrutton, N. S. (1999) *Biochemistry 38*, 3218−3222.
18. Basran, J., Patel, S., Sutcliffe, M. J., and Scrutton, N. S. (2001) *J. Biol. Chem. 276*, 6234−6242.
19. Grant, K. L., and Klinman, J. P. (1989) *Biochemistry 28*, 6597−6605.
20. Bahnson, B. J., and Klinman, J. P. (1995) *Methods Enzymol. 249*, 373−397.
21. Basran, J., Sutcliffe, M. J., and Scrutton, N. S. (2001) *J. Biol. Chem. 276*, 24581−24587.
22. Harris, R. J., Meskys, R., Sutcliffe, M. J., and Scrutton, N. S. (2000) *Biochemistry 39*, 1189−1198.
23. Seymour, S., and Klinman, J. P. (2002) *Biochemistry 41*, 8747−8758.
24. Kohen, A., Cannio, R., Bartolucci, S., and Klinman, J. P. (1999) *Nature 399*, 496−499.
25. Northrop, D. B., and Cho, Y. K. (2000) *Biochemistry 39*, 2406−2412.
26. Knapp, M. J., Rickert, K., and Klinman, J. P. (2002) *J. Am. Chem. Soc. 124*, 3865−3874.
27. Francisco, W. A., Knapp, M. J., Blackburn, N. J., and Klinman, J. P. (2002) *J. Am. Chem. Soc. 124*, 8194−8195.
28. Schowen, R. (2002) *Eur. J. Biochem. 269*, 3095.
29. Sutcliffe, M. J., and Scrutton, N. S. (2002) *Eur. J. Biochem. 269*, 3096−3102.
30. Knapp, M. J., and Klinman, J. P. (2002) *Eur. J. Biochem. 269*, 3113−3121.
31. Antoniou, D., Caratzoulas, S., Kalyanaraman, C., Mincer, J., and Schwartz, S. (2002) *Eur. J. Biochem. 269*, 3103−3112.
32. Bruno, W. J., and Bialek, W. (1992) *Biophys. J. 63*, 689−699.
33. Kuznetsov, A. M., and Ulstrup, J. (1999) *Can. J. Chem. 77*, 1085−1096.
34. Faulder, P. F., Tresadern, G., Chohan, K. K., Scrutton, N. S., Sutcliffe, M. J., Hillier, I. H., and Burton, N. A. (2001) *J. Am. Chem. Soc. 123*, 8604−8605.
35. Alhambra, C., Sanchez, M. L., Corchado, J. C., Gao, J., and Truhlar, D. G. (2001) *Chem. Phys. Lett. 347*, 512−518.
36. Bahnson, B. J., Park, D.-H., Kim, K., Plapp, B. V., and Klinman, J. P. (1993) *Biochemistry 32*, 5503−5507.
37. Bahnson, B. J., Colby, T. D., Chin, J. K., Goldstein, B. M., and Klinman, J. P. (1997) *Proc. Natl. Acad. Sci. U.S.A. 94*, 12797−12802.
38. Lehman, T. C., Hale, D. E., Bhala, A., and Thorpe, C. (1990) *Anal. Biochem. 186*, 280−284.
39. Beardmore-Gray, M., O'Keffe, D. T., and Anthony, C. (1983) *J. Gen. Microbiol. 129*, 923−933.
40. Armstrong, J. (1964) *Biochim. Biophys. Acta 86*, 194−197.
41. Davidson, V. L., Wu, J., Miller, B., Jones, L. H. (1992) *Biochemistry 31*, 1504−1508.
42. Goodwin, M. G., and Anthony, C. (1996) *Biochem. J. 318*, 673−679.
43. Afolabi, P. R., Mohammed, F., Amaratunga, K., Majekodunmi, O., Dales, S. L., Gill, R., Thompson, D., Cooper, J. B., Wood, S. P., Goodwin, P. M., and Anthony, C. (2001) *Biochemistry 40*, 9799−9809.
44. Strickland, S., Palmer, G., and Massey, V. (1975) *J. Biol. Chem. 250*, 4048−4052.
45. Goodford, P. J. J. (1985) *J. Med. Chem. 28*, 849−857.
46. Itoh, S., Mure, M., Ogino, M., and Oshiro, Y. (1991) *J. Org. Chem. 56*, 6857−6865.

BI027282V